

Ixora coccinea – As an Environmentally Viable Corrosion Inhibitor for Mild Steel in 1 M HCl

A. Prithiba¹, S. Manimegalai^{2*}

¹Department of Chemistry, Avinashilingam Institute for Home Science and Higher Education for Women, Coimbatore, Tamil Nadu, India, ²Department of Chemistry, Arulmigu Palaniandavar College of Arts and Culture, Palani, Tamil Nadu, India

ABSTRACT

Corrosion inhibitors for acid cleaning process are used to restrict dissolution of the base metal and decrease acid consumption and hydrogen gas evolution. Because of the toxic nature and high cost of some chemicals currently in use, it is necessary to develop environmentally acceptable and less expensive inhibitors. Natural products can be considered as a good source for this purpose. The present study of the effective performance of acid extract of *Ixora coccinea* on the corrosion inhibition of mild steel in 1 M HCl at ambient temperature has been carried out as an eco-friendly initiative to mitigate corrosion of mild steel in acid medium. Conventional mass loss and electrochemical measurement techniques were used for the experimental purpose. Experiments were carried out by varying the concentration of the extract in different period of immersion and at different temperatures. Suitable adsorption isotherm was obtained. Thermodynamic and kinetic parameters were evaluated. Electrochemical measurements inferred mixed mode of inhibition. Surface analytical techniques such as FT-IR, UV-Visible, SEM, and 3D Optical Profilometer proved the corrosion inhibitive property of the investigated inhibitor.

Key words: Green inhibitor, Mild steel, Electrochemical measurements, Thermodynamic parameters and surface analytical techniques.

1. INTRODUCTION

Corrosion inhibition of mild steel is a matter of theoretical as well as practical importance. It has been widely used in industries such as pickling, cleaning, and descaling, and because of their aggressiveness and inhibitors is used to reduce the dissolution of metals [1-3]. Many organic heterocyclic compounds containing N, S, O, and P have been reported as inhibitors [4-6]. A large number of organic compounds have been used as corrosion inhibitors for mild steel and most of them are highly toxic to both human beings and environment. Due to the increasing environmental awareness and the negative effects of some chemicals, research activities in recent times are geared toward developing the less toxic and environmentally safe corrosion green inhibitors [7-10].

Natural products of plant origin contain various organic compounds such as alkaloids, flavonoids, terpenoids, saponins, primary and secondary alcohols, quinones, fatty acids, steroids, and other minor components. Commonly, the inhibitive effect of plant extract is attributed to adsorption of organic substances on the metal surface therefore blocking active site or even forming a protective barrier [11-13]. The main objective of the present study was to select an eco-friendly, cost-effective, naturally occurring plant material such as *Ixora coccinea* leaf extract as corrosion inhibitor for mild steel in acidic medium.

2. MATERIALS AND METHODS

2.1. Plant Inhibitor

I. coccinea (Family – Rubiaceae) is a dense, multibranched evergreen shrub, commonly 4–6 ft (1.2–2 m) in height. The anticancer activity of the leaves of *I. coccinea* of main constituent's compound was found

to be due principally to the known alkaloid, camptothecin [14]. The structure of camptothecin is shown in Figure 1.

2.2. Selection and Preparation of Metal, Test Medium, and Inhibitor

Regular sample of area $1 \times 5 \text{ cm}^2$ has been cut from a large sheet of mild steel. A hole was drilled in the specimen, mechanically polished, degreased, washed with deionized water then thoroughly dried, and kept in desiccator for weight loss tests. The extract was prepared by refluxing 25 g of *I. coccinea* leaves in 500 ml of HCl for 3 h and kept overnight for cooling. The cooled extract was filtered and made up to 500 ml with 1 M HCl to get 5% v/v extract of inhibitor.

2.3. Experimental Methods

Pre-weighed coupons were immersed in triplicate with the help of glass hook into a beaker containing 100 ml of 1 M HCl with and without inhibitor for a particular period of time. The coupons were then washed, dried, and reweighed. The average weight loss of coupons was recorded. The corrosion rate was determined using the following equation:

$$\text{C.R (mpy)} = 543 \times W/D \times A \times T \quad (1)$$

*Corresponding author:

E-mail: mani_megalai22@yahoo.in

ISSN NO: 2320-0898 (p); 2320-0928 (e)

DOI: 10.22607/IJACS.2021.903013

Received: 17th July 2021

Revised: 04th August 2021

Accepted: 17th August 2021

Where, W – Weight loss in g, D – Density of mild steel in g/cm^2 , A – Area of the sample in cm^2 , and T – Exposure time in hours. The change in free energy (ΔG) of adsorption of the inhibitors can be calculated using the following equation,

$$\log C = [\log \theta/(1-\theta)] - \log B \quad (2)$$

Where, $\log B = -1.74 - (\Delta G/2.303 RT)$, θ is the surface coverage, C is the concentration of inhibitor, R is the gas constant $8.314 \text{ J}/\text{mol}$, and T is the temperature in K. The value of enthalpy of adsorption ΔH and entropy of adsorption ΔS were obtained from the basic thermodynamic equation.

$$\Delta G = \Delta H - T\Delta S \quad (3)$$

The activation energy (E_a) was calculated using the following formula.

$$E_a = -2.303 \times R \times \text{Slope of the Arrhenius plot} \quad (4)$$

The values of activation parameters – ΔH_a and ΔS_a were calculated using

$$\ln CR = RT/Nh \exp(\Delta S_a/R) \exp(\Delta H_a/R) \quad (5)$$

Where, h is Planck's constant, N is Avogadro number, ΔS_a is entropy of activation, and ΔH_a is enthalpy of activation.

2.4. Electrochemical Methods – Polarization Techniques

Electrochemical studies were carried out using conventional three electrode cells with large area of platinum foil as counter electrode saturated calomel electrode as reference electrode and sample was as working electrode. Electrochemical measurements were done using Biologic EC Lab software version 10.23.

2.5. Linear Polarization Measurements

Before starting the measurements, the electrode potential was allowed to stabilize for 30 min. Polarization studies were conducted at a scan rate of $2 \text{ mV}/\text{sec}$ from -0.1 to -1 mV with respect to the corrosion potential in the presence and absence of the inhibitor. One sq. cm. of polished mild steel surface was exposed, and the electrochemical studies were carried out at 303 K .

2.6. Impedance Spectroscopy

In this method, an AC signal of $5-10 \text{ mV}$ of frequency $10 \text{ KHz}-10 \text{ MHz}$ is applied to the system. Impedance data can be presented in the form of Nyquist or Bode plot. From the data, the R_{ct} and C_{dl} are obtained.

2.7. Surface Analytical Techniques

The FT-IR spectrum was recorded for leaves of ICL extract with a frequency ranging from 4000 to 400 cm^{-1} using PerkinElmer FT-IR spectrophotometer with the SOFTWARE – OPUS version 6.5. UV-visible absorption spectrophotometric method was carried out on the prepared metal samples after immersion in 1 M HCl with and without

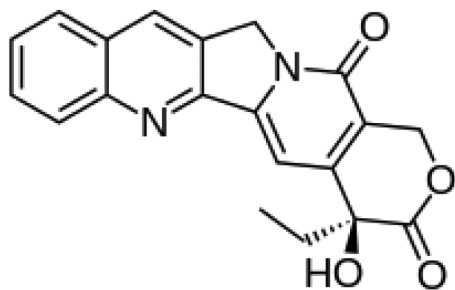


Figure 1: Structure of camptothecin

addition of 0.7% inhibitor for 3 h . Scanning electron microscopy (SEM) JEOL MODEL JSM 6360 was used to examine the morphology of the metal surface in the presence and absence of inhibitors. Surface profiles and pores were studied using a Zeta-20 3D Optical Profiler. MS specimens – plain and after exposure to 1 M HCl solution in the absence and presence of ICL extract for 3 h were mounted on sample holder occurred under the objective of the Optical Profiler and the 3D photos were taken from the $\times 100$ magnified surface through operating program on computer.

3. RESULTS AND DISCUSSION

3.1. Mass Loss Studies – Effect of Concentration and Immersion Time on I. coccinea Leaf Extract in 1 M HCl

The IE of mild steel exposed to 1 M HCl at room temperature ($30 \pm 2^\circ\text{C}$) as a function of different concentrations of the inhibitor and time of immersion is shown in Figure 2 and Table 1. It is observed that the inhibition efficiency of mild steel increased with increasing concentrations of inhibitors. This behavior could be attributed to the increase in adsorption of inhibitors on the metal or at the solution interface on increasing its concentration. The highest % IE was 96.95 at 0.7 concentration of the extract. The plant extract was seen to reduce the corrosion rate at all studied concentrations indicating inhibition of the corrosion reaction [15].

The results also indicated that as the immersion period increased, the IE was also found to increase with $93.9-96\%$ for $1/2-3 \text{ h}$. However, it slightly decreased in 6 h . Then, the IE stabilized at 24 h to yield efficiency 97% [16].

3.2. Role of Temperature

The influence of temperature on ICL extract was tested in 1 M HCl solution at different temperatures (Table 2). It has been found that the corrosion rate increased with the increase in temperature for the inhibitor. The corrosion rate of MS in the absence of inhibitor increased steeply from 303 K to 353 K . However, in the presence of inhibitor, the corrosion rate increased slowly [17].

3.3. Adsorption Isotherms

Adsorption isotherms were employed in this study to investigate which of two main types of interaction such as chemisorption (or) physisorption describes the interaction between the mild steel and ICL extract molecules. Linear plots of $\log \theta/(1-\theta)$ against the $\log C$

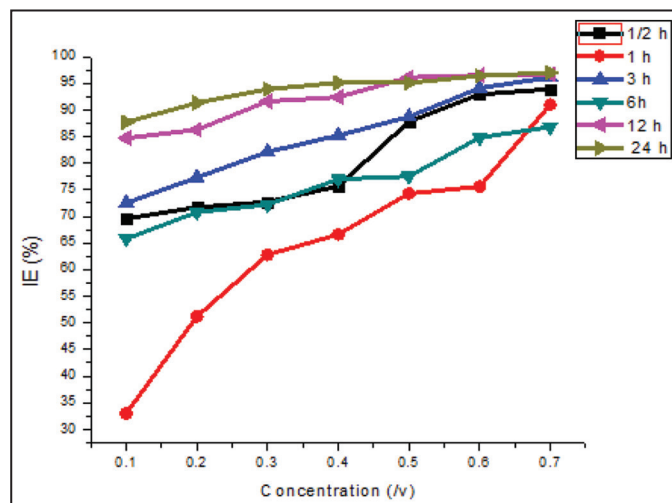


Figure 2: Effect of conc. and immersion time on the inhibition efficiency of ICL in 1 M HCl

Table 1: Role of concentration and immersion time of ICL extract on MS in 1 M HCl

S. No.	Conc. (%)	Corrosion rate and inhibition efficiency											
		½ h		1 h		3 h		6 h		12 h		24 h	
		CR (mpy)	IE (%)	CR (mpy)	IE (%)	CR (mpy)	IE (%)	CR (mpy)	IE (%)	CR (mpy)	IE (%)	CR (mpy)	IE (%)
1.	Blank	844	-	332	-	864	-	253	-	532	-	379	-
2.	0.1	255	69.6	221	33	237	72.5	86	65.8	81	84.7	46	87.7
3.	0.2	243	71.7	162	51.2	196	77.3	73	70.8	72	86.3	33	91.3
4.	0.3	230	72.7	123	62.8	154	82.1	70	72.2	44	91.6	23	93.9
5.	0.4	204	75.7	102	66.6	127	85.2	58	77.0	40	92.4	18	95.1
6.	0.5	102	87.8	85	74.3	98	88.7	56	77.5	20	96.1	18	95.1
7.	0.6	59	92.9	81	75.6	51	94.1	38	84.8	18	96.5	13	96.4
8.	0.7	34	93.9	29	91.0	34	96.1	33	86.8	17	96.7	11	97.0

Table 2: Impact of temperature on corrosion of MS in the presence of various concentration of ICL extract in 1 M HCl

S. No.	Conc. (%)	Corrosion rate and inhibition efficiency											
		303 K		313 K		323 K		333 K		343 K		353 K	
		CR (mpy)	IE (%)	CR (mpy)	IE (%)	CR (mpy)	IE (%)	CR (mpy)	IE (%)	CR (mpy)	IE (%)	CR (mpy)	IE (%)
1.	Blank	844	-	2021	-	3997	-	5416	-	12401	-	33862	-
2.	0.1	255	69.6	1032	48.9	989	73.0	1705	68.5	2840	77.0	10721	68.3
3.	0.2	243	71.7	716	64.5	887	75.8	1535	71.6	2729	77.9	7565	77.6
4.	0.3	230	72.7	622	69.1	673	81.6	1458	73.0	2644	78.6	5885	82.6
5.	0.4	204	75.7	204	89.8	656	82.0	1134	79.0	2490	79.9	5697	83.1
6.	0.5	102	87.8	145	92.8	469	87.2	1100	79.6	1970	84.1	4546	86.5
7.	0.6	59	92.9	59	97.0	435	88.1	938	82.6	1629	86.8	2942	91.3
8.	0.7	34	93.9	51	97.4	417	88.6	477	91.1	1134	90.8	2601	92.3

were obtained with the slope in the range of which is close to unity in Figure 3. These results suggest that the inhibitor occupies the adsorption sites on the metal surface. Besides, the results show that all the linear correlation coefficients (R^2) were almost equal to unity. Thus, the adsorption phenomenon of inhibitor into the mild steel surface obeys the Langmuir isotherm.

3.4. Activation Energy

The value of apparent activation energy (E_a) for the corrosion process was calculated from Arrhenius plot of $\log CR$ versus $1/T$ in the absence and presence of inhibitor, as shown in Figure 4.

The values of E_a obtained from the slopes of these straight lines are recorded in Table 3. The values of E_a were higher for inhibited solutions indicating physical adsorption of the inhibitor on the metal surface [18]. A plot of $\log CR/T$ against $1/T$ yielded straight line is shown in Figure 5 with a slope of $(-\Delta H_a/2.303R)$ and an intercept of $(\log (R/Nh) + (\Delta S_a/2.303R))$.

The values of E_a and ΔH_a were close to each other as expected from the concept of transition state theory and vary in the same manner on the addition of different concentrations of inhibitor. Therefore, all values were of endothermic nature due to iron dissolution. The positive sign of ΔH_a may be contributed to the endothermic nature of the MS dissolutions process. The higher values of ΔS_a for inhibited solutions may contribute to the increase in solvent entropy. The negative value of ΔS_a for ICL in HCl indicates that activated complex in the rate

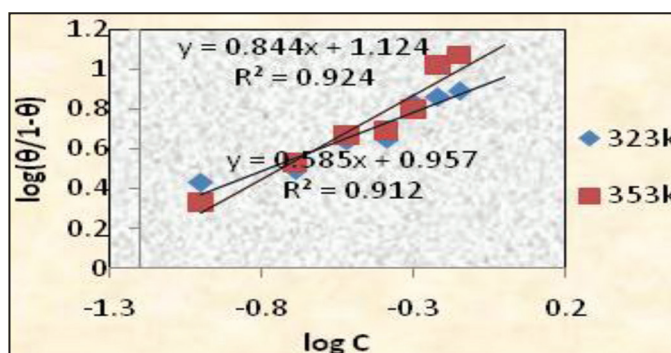


Figure 3: Langmuir adsorption isotherm for MS/HCl/ICL extract

determining step represents an association compared to dissociation step. That means, a decrease in disorderliness, that is, entropy takes place during the transition from reactants to the activated complex [19].

3.5. Thermodynamic Parameters

For all the systems studied in 1 M HCl medium, the value of ΔG increases with increase in concentration and increases with increase in temperature and ΔG_{ads} values range from $-14KJ/mol$ to $-21 KJ/mol$ from 303 K to 353 K (Table 4 and Figure 6). Thermodynamic parameters ΔH_{ads} and ΔS_{ads} could be arrived at from the temperature studies and using a plot of $-\Delta G$ versus T. The negative values of ΔH_{ads} also

show that the adsorption of inhibitor is an exothermic process. In an exothermic process, physisorption is distinguished from chemisorption by considering the absolute value of a physisorption process lower than 40 kJ mol⁻¹ while the adsorption heat of a chemisorption process approaches 100 kJ mol⁻¹. The adsorption of inhibitor molecules was accompanied by positive values of ΔS_{ads}.

3.6. Electrochemical Measurements

3.6.1. Polarization techniques

Linear polarization measurements, Tafel intercept method, and electrochemical impedance measurements were carried out for mild steel acid corrosion in the presence of ICL extract. The values of corrosion kinetic parameters – corrosion current (E_{corr}), current density (I_{corr}), Tafel slope constants (b_a and b_c), and linear polarization resistance (R_p) are recorded in Table 5 and Figure 7. The inhibition efficiency was calculated using the following equation,

$$IE (\%) = \frac{I_{corr}(\text{blank}) - I_{corr}(\text{inhibited})}{I_{corr}(\text{blank})} \times 100 \quad (6)$$

$$IE (\%) = \frac{R_p(\text{inhibited}) - R_p(\text{blank})}{R_p(\text{inhibited})} \times 100 \quad (7)$$

I.E from LPR technique,

From Table 5, it can be inferred that the values of corrosion current density I_{corr} decreased with increasing concentration of the inhibitor. Noticeable change was not observed in E_{corr} values. The values of Tafel slopes (b_a and b_c) changed with increasing concentration of the ICL extract indicating that the extract acted mixed type by controlling the cathodic hydrogen evolution as well as anodic metallic dissolution.

Table 3: Values of E_a , ΔH_a , and ΔS_a of MS in various concentrations of ICL extract in 1 M HCl medium

S. No.	Conc. V/V (%)	Activation energy- E_a kJ/mol	ΔH_a kJ/mol	ΔS_a kJ/mol
1.	Blank	61.02	58.37	3.27
2.	0.1	56.36	53.45	-21.46
3.	0.2	54.79	52.19	-26.73
4.	0.3	53.61	51.08	-31.21
5.	0.4	62.26	59.37	-8.12
6.	0.5	69.86	74.06	30.84
7.	0.6	76.55	67.16	13.03
8.	0.7	78.92	76.32	35.05

Values of E_{corr} indicate that the ICL extract behaved as mixed type inhibitor. The values of R_p increased with increase in concentration of the ICL extract for both 1 M HCl. Decrease in I_{corr} values and increase in R_p values with increase in concentration of extract revealed that the

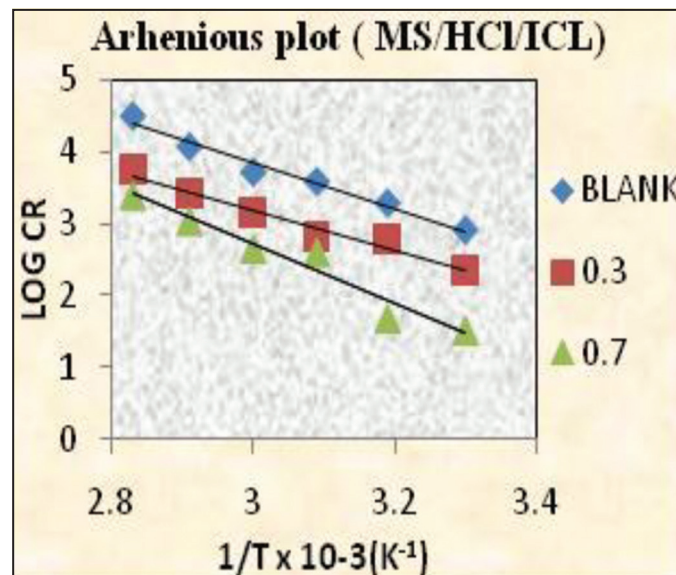


Figure 4: Arrhenius plot

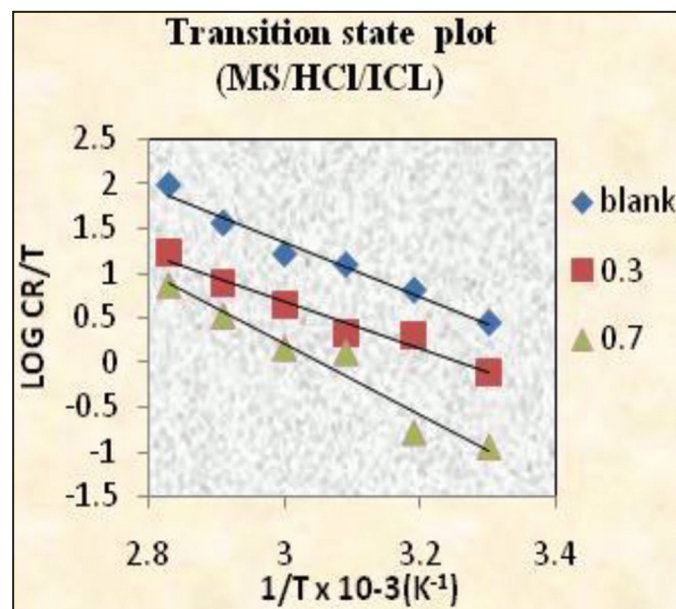


Figure 5: Transition state plot

Table 4: Values of $-\Delta G$, ΔH , and ΔS of MS in various concentration of ICL 1 M HCl

S. No.	Concentration of inhibitor V/V (%)	Free energy of adsorption $-\Delta G$ (kJ/mol)						ΔS (J/mol)	ΔH (kJ/mol)
		303 K	313 K	323K	333 K	343 K	353K		
1.	0.1	17.98	16.30	19.61	19.62	21.44	20.77	8.38	-8.21
2.	0.2	16.49	16.17	18.15	18.11	19.61	20.13	8.13	-8.57
3.	0.3	15.59	15.65	17.99	17.18	18.57	19.86	8.36	-9.96
4.	0.4	15.26	18.47	17.29	17.30	17.97	19.12	5.08	0.88
5.	0.5	16.81	18.88	17.77	16.78	18.15	19.24	2.56	9.52
6.	0.6	17.86	20.80	17.51	16.82	18.25	20.16	9.04	15.60
7.	0.7	17.88	20.78	17.22	18.52	18.97	20.09	1.98	12.40

Table 5: Electrochemical polarization parameters for the corrosion of MS in the presence of ICL extract in 1 M HCl

S. No.	Conc. v/v (%)	-E _{corr} mV/saturated calomel electrode	I _{corr} μA/cm ²	b _a mV/dec	b _c mV/dec	IE (%)	R _p (Ω/cm ²)	IE (%)
1	Blank	-479.7	530.7	93.8	150.5	-	55.4	-
2	0.3	-478.0	85.2	74.6	190.3	83.9	269	79.4
3	0.7	-456.7	28.3	52.9	153.6	94.6	491	88.7

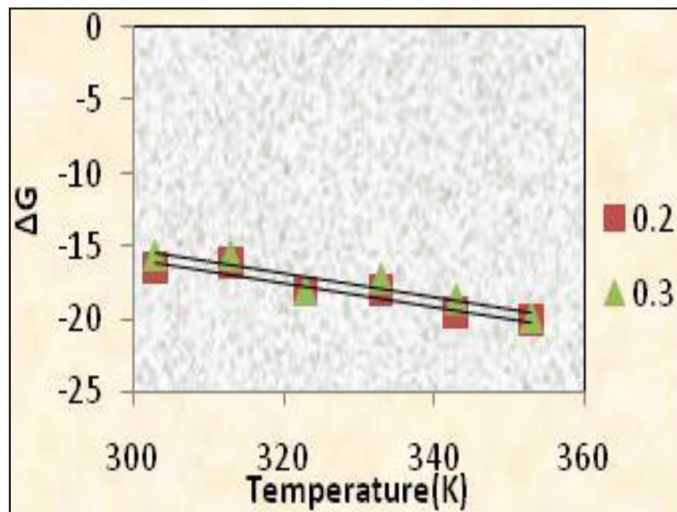


Figure 6: Plot of ΔG versus temperature for ICL extract in 1 M HCl

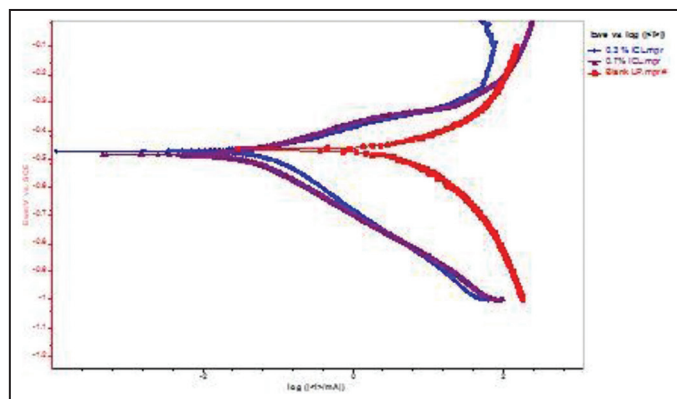


Figure 7: Potentiodynamic polarization plots for MS in 1 M HCl in the presence and absence of ICL extract

inhibition process was taking place by adsorption of the extract on mild steel. Inhibition efficiency calculated using I_{corr} and R_p indicates that inhibition efficiency increased with increase in concentration of the extract and maximum inhibition efficiency was found to be 88.7% using R_p values and 94.6% using I_{corr} values [20].

3.6.2. Electrochemical impedance spectroscopy

Nyquist representations of the impedance with and without the addition of ICL are given in Figure 8. The Nyquist plots were depressed semi circles with centers below the real axis. This indicated that the corrosion process was charge transfer controlled. The corrosion parameters obtained are presented in Table 6. The charge transfer resistance (R_{ct}) increased with inhibitor concentration. The inhibition efficiency was calculated using the Equation (8).

$$IE (\%) = \frac{R_{ct}(\text{inhibited}) - R_{ct}(\text{blank})}{R_{ct}(\text{inhibited})} \times 100 \quad (8)$$

Table 6: R_s, R_{ct}, C_{dl}, and IE of MS in the presence of ICL extract in 1 M HCl

S. No.	Conc. (%)	R _s	R _{ct} (Ω cm ²)	IE (%)	C _{dl} (F/cm ²)	θ
1	Blank	6.28	81.1	-	107	-
2	0.3	-3.29	526	84.5	55.15	0.4845
3	0.7	14.72	654.3	87.6	44.34	0.5856

R_{ct} (inhibited) and R_{ct} (blank) are charge transfer resistance in the presence and absence of the inhibitor, respectively. With the help of the double-layer capacitance C_{dl}, θ can be calculated using the following equation,

$$\theta = \frac{1 - C_{dl}(\text{inhibited})}{C_{dl}(\text{blank})} \times 100 \quad (9)$$

Where, C_{dl} (inhibited) and C_{dl} (blank) are the double-layer capacitance in the presence and absence of the inhibitor, respectively.

Maximum inhibition efficiency using R_{ct} values was found to be 87.6% at 0.7%. concentration. The large charge transfer resistance could be due to a decrease in the active surface necessary for the corrosion reaction [21]. The recorded EIS spectrum of mild steel in 1 M HCl solution without and with 0.7% ICL extract showed one depressed capacitive loop at low frequencies. The high-frequency semicircle was attributed to the time constant of charge transfer and double-layer capacitance. The low-frequency inductive loop may be attributed to the relaxation process obtained by adsorption species such as Cl⁻_{ads} and H⁺_{ads}. As shown in Figure 8, only 1 time constant was detected on the Bode plots for the blank and 0.7 concentrations. The value of C_{dl} decreased with increase in inhibitor concentration thus the thickness of protective layer increased. This may be attributed to the decrease in local dielectric constant and an increase in the thickness of the electrical double layer suggesting that ICL inhibited the mild steel corrosion by adsorption at the metal/acid interface [22].

3.7. Surface Analysis

3.7.1. FT-IR spectral analysis of ICL extract and corrosion products in 1 M HCl

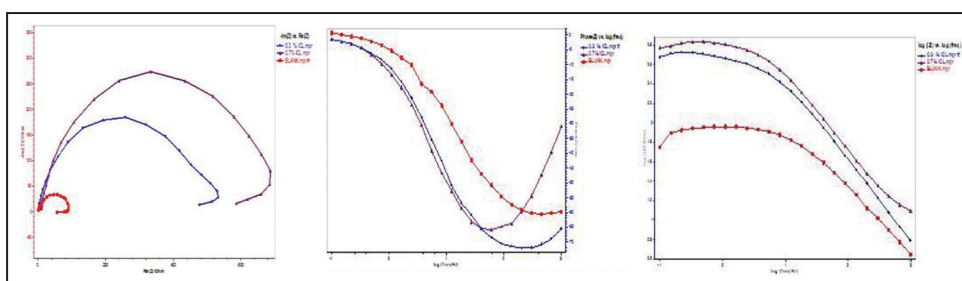
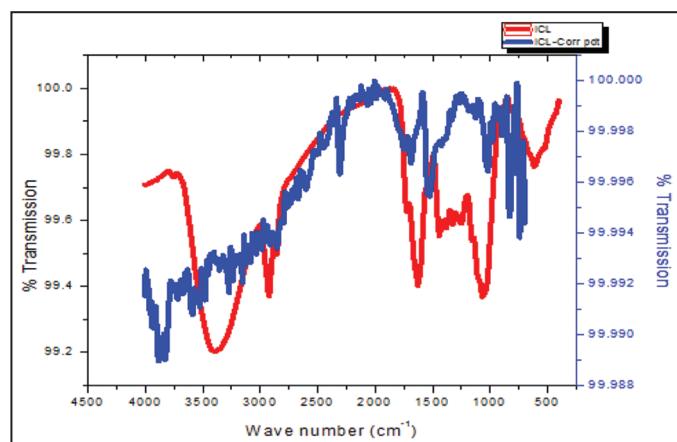
The comparison of IR frequencies of ICL extract and corrosion products is tabulated in Table 7 and represented in Figure 9. The shift in the absorption frequencies of the inhibitor on the metal surface strongly supports the interaction between the phytochemical compounds of the inhibitor and metal surface. The band at 450 cm⁻¹ to 800 cm⁻¹ probably originates mainly from γ-Fe₂O₃ (740.67 cm⁻¹). Some missing bonds are there in corrosion products indicating that there is interaction (Fe-complex formation) between the leaves extract of and the surface of mild steel.

3.7.2. UV analysis of ICL extract and corrosion products in 1 M HCl

To confirm the possibility of the formation of inhibitor-Fe complex, UV-Visible absorption spectra obtained from 1 M HCl solution containing ICL extract before and after the mild steel immersion are

Table 7: IR spectrum of (a) acid extract of ICL (b) adsorbed material of MS in the presence of ICL

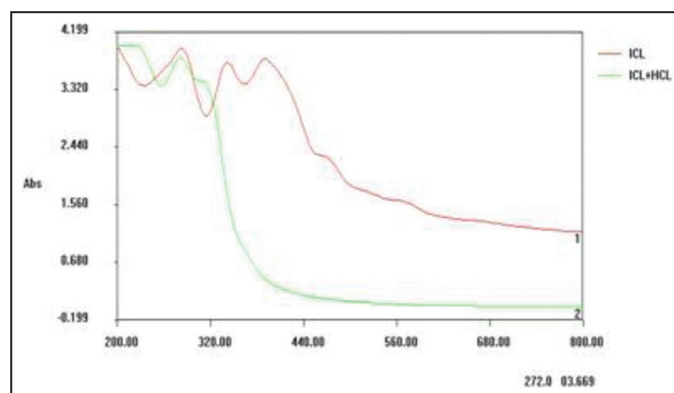
Powdered plant material			Corrosion product of MS in ICL		
Frequency cm^{-1}	Assignment	Functional Groups	Frequency cm^{-1}	Assignment	Functional groups
3395	OH stretch	Alcohol	3480	O–H stretch, H–bonded	1°, 2° amines, amides
2924	C–H stretch	Alkanes	2986	C–H stretch	Alkanes
2376	-C≡N stretch	Aliphatic amines	2307	-C≡N stretch	Aliphatic amine
1628	C=O stretch	Carbonyl groups, acids, esters, ethers	1690	C=O stretch	Carbonyl groups, carboxylic acids, esters, ethers
1443	C–H bend	Aliphatic amines	1528	C-C in ring	Aromatics
1327	C–O–C stretch	Ethers	1427	C–H bend	Aliphatic amines
1250	C–O stretch	carboxylic acids	-	-	-
1065	C–O stretch	carboxylic acids	1018	C–O stretch	carboxylic acids
772	O–H bend	Alcohols	779	O–H bend	Alcohols
			741	- γ -Fe ₂ O ₃	-

**Figure 8:** Impedance plots in Nyquist and Bode format for MS in 1 M HCl in the presence and absence of ICL extract**Figure 9:** IR spectrum of ICL extract and corrosion products in 1 M HCl

shown in Figure 10. The electronic absorption spectra of ICL before immersion have absorption maximum at 282, 389, and 342 nm which can be attributed to π - π^* and n - π^* transitions. After 3 h immersion of mild steel, the change in the position of absorption maximum or the change in the absorbance values to 284 and 318 nm indicates the complex formation between two species in solution. These experimental findings provide the formation of complex between Fe^{2+} and Fe^{3+} and confirm the inhibition of mild steel from corrosion [23].

3.7.3. SEM analysis of ICL extract and corrosion products in 1 M HCl

Surface morphology of MS was studied by SEM after 3 h immersion in 1 M HCl before and after addition of 0.7% ICL. Figure 11a represents

**Figure 10:** UV spectrum of ICL extract in 1 M HCl

the micrograph obtained of polished MS without being exposed to the corrosive environment while Figure 11b shows strongly damaged MS surface due to the formation of corrosion products after immersion in 1 M HCl solution. It could be seen that no pits and cracks were observed in the micrographs after immersion of MS in 1 M HCl in the presence of 0.7% ICL except polishing lines (Figure 11c). Thus, it revealed the presence of a good protective film on adsorption of inhibitor molecules onto the MS surface, which was responsible for the inhibition of corrosion [24].

3.7.4. 3D optical profilometer

The technique was employed to reveal the surface microstructure of metal after corrosion test. From the technique, average roughness Ra and root mean square values can be determined. Figures 12-14 display the three-dimensional image of mild steel surface immersed in 1 M HCl solution without and with addition of 0.7% ICL for 3 h. Table 8

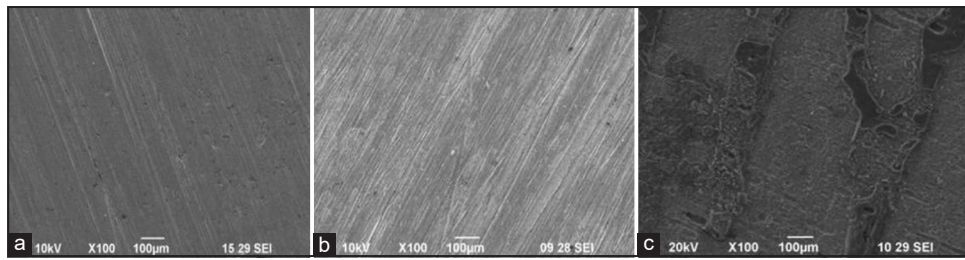


Figure 11: (a) Plain MS. (b) MS in 1 M HCl. (c) 1 M HCl + 0.7% ICL

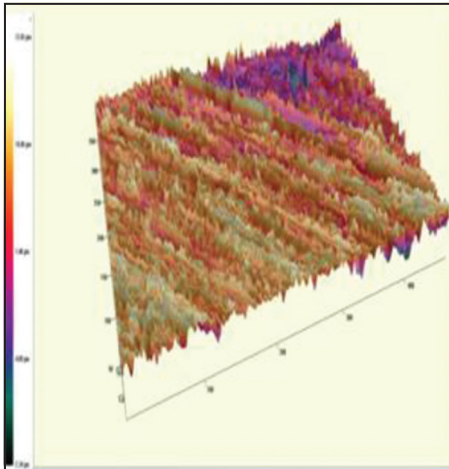


Figure 12: Plain MS

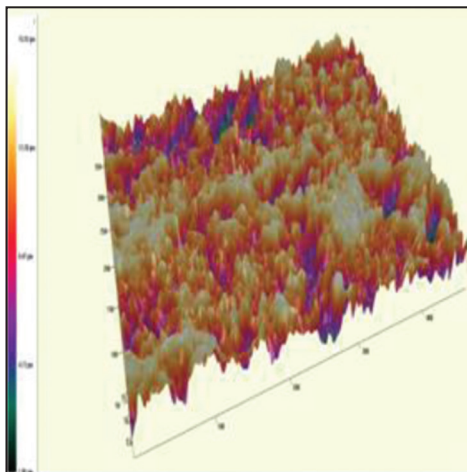


Figure 13: MS in 1 M HCl

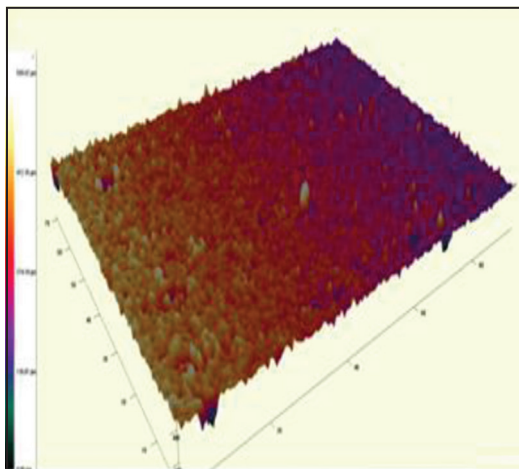


Figure 14: MS in 1 M HCl + 0.7% ICL

Table 8: Ra and Rq values for MS/1 M HCl /ICL extract

Samples	Average roughness Ra (μm)	Root mean square roughness Rq (μm)
Plain MS	2.558	3.140
MS in 1 M HCl	17.28	22.35
MS in 1 M HCl + 0.7% ICL	9.20	12.57

gives the corresponding average roughness Ra and RMS roughness (Rq) values. By contrast, the corrosion morphology of mild steel in uninhibited 1 M HCl solution is about 17.28 μm and Rq is 22.35 μm because of the acid attack, while in the presence of ICL, Ra and Rq decrease to 8.48 and 12.14 μm , respectively. This indicates that the addition of the extract reduced the surface roughness. 3D optical profilometer images and the roughness quantification are also consistent with SEM studies. This confirms that the corrosion inhibition on mild steel occurs through adsorption of the extract on it [25].

3.8. Mechanism of Inhibition

In general, the first stage in the corrosion inhibition mechanism is the adsorption of inhibitor molecules on the mild steel surface. The process of adsorption is influenced by the type of the aggressive electrolyte, the chemical structure of the inhibitor molecules, and the nature and charge of the metal. The charge on the metal surface is due to the electric field generated at the metal/electrolyte interface. It is reported that in acid solutions, the mild steel surfaces are positively charged with respect to their potential zero charge (PZC) [26]. ICL may adsorb on the mild steel surface by (i) electrostatic interaction of the inhibitor molecules with already adsorbed chloride ions (physisorption), (ii) vacant d-orbitals of metal surface atoms and unshared electron pairs of heteroatoms (chemisorption), or (iii) interaction of vacant the d-orbital of the inhibitor molecule with the d-electron of the metal surface (retro-donation).

In acidic medium, the phytochemicals present in ICL molecules may adsorb through protonated heteroatoms (N, O, and S) and already adsorbed anions on the mild steel surface. Initially, the protonated forms of ICL molecules in acid medium compete with H⁺ ions for electrons on the mild steel surface. The high electron density on the mild steel surface renders more negative charge to it. To relieve the surface from the high negative charge, the electron from the d-orbital of Fe may be transferred to the vacant π^* -orbital (anti-bonding) of the ICL molecules and in turn strengthens their adsorption on the mild steel surface [27,28].

4. CONCLUSION

The evaluation of the effective performance of acid extract of ICL on the corrosion inhibition of mild steel in 1 M HCl at room and higher

temperature was made. Inhibition efficiency increased with increase in concentration both at room temperature and at higher temperature in 1 M HCl medium. Inhibition efficiency was found to be increasing with increase in temperature up to 313 K. Experimental results fitted well into Langmuir and Temkin isotherm. Values of activation energy infer the strong adsorption of inhibitor molecules on mild steel surface. Thermodynamic parameters showed that the inhibition was spontaneous physical adsorption of inhibitors on mild steel surface. Polarization curves obtained in the presence of ICL extract indicate that it controls both anodic and cathodic reactions. Increase in R_p and R_{ct} values and decrease in I_{corr} and C_{dl} values confirm that the extract is adsorbed on the mild steel surface and the inhibition process is followed by monolayer adsorption.

Surface analysis such as FT-IR, UV-Visible, SEM, and 3D optical profilometer further reaffirmed the effect of ICL on minimizing the corrosion of mild steel. Therefore, the study on corrosion inhibition of mild steel in the presence of ICL extract could reduce the pollution problems and the inhibitor could act definitely as environmentally friendly corrosion inhibitor.

REFERENCES

1. S. A. Ali, M. T. Saeed, S. V. Rahman, (2003) The isoxazolidines: A new class of corrosion inhibitors of mild steel in acidic medium, *Corrosion Science*, **45**: 253-266.
2. M. Lagrenee, B. Mernari, M. Bouanis, M. Traisnel, F. Bentiss, (2002) Study of the mechanism and inhibiting efficiency of 3, 5-bis (4-methylthiophenyl)-4H-1, 2, 4-triazole on mild steel corrosion in acidic media, *Corrosion Science*, **44**: 573-588.
3. M. A. Quraishi, R. Sardar, (2002) Aromatic triazoles as corrosion inhibitors for mild steel in acidic environments, *Corrosion*, **58**: 748-755.
4. M. A. Quraishi, M. Athar, H. Ali, (2002) Corrosion inhibition of carbon steel in hydrochloric acid by organic compounds containing hetero atoms, *British Corrosion Journal*, **37**: 155-158.
5. M. A. Quraishi, F. A. Ansari, (2003) Corrosion inhibition by fatty acid triazoles for mild steel in formic acid, *Journal of Applied Electrochemistry*, **33**: 233-238.
6. M. A. Quraishi, S. Khan, (2006) Inhibition of mild steel corrosion in sulfuric acid solution by thiadiazoles, *Journal of Applied Electrochemistry*, **36**: 539-544.
7. S. K. Shukla, M. A. Quraishi, (2010) Cefalexin drug: A new and efficient corrosion inhibitor for mild steel in hydrochloric acid solution, *Materials Chemistry and Physics*, **120**: 142-147.
8. S. M. Megalai, P. Manjula, K. N. Manonmani, N. Kavitha, N. Baby, (2012) metronidazole: A corrosion inhibitor for mild steel in aqueous environment, *Portugaliae Electrochimica Acta*, **30**: 395-403.
9. M. S. Morad, (2008) Inhibition of iron corrosion in acid solutions by cefatrexyl: Behaviour near and at the corrosion potential, *Corrosion Science*, **50**: 436-448.
10. S. K. Shukla, M. A. Quraishi, (2009) Cefotaxime sodium: A new and efficient corrosion inhibitor for mild steel in hydrochloric acid solution, *Corrosion Science*, **51**: 1007-1011.
11. E. E. Oguzie, (2008) Corrosion inhibitive effect and adsorption behaviour of *Hibiscus sabdariffa* extract on mild steel in acidic media, *Portugaliae Electrochimica Acta*, **26**: 303-314.
12. P. R. Vijayalakshmi, R. Rajalakshmi, S. Subhashini, (2010) *Cocos Nucifera* shell as a potential inhibitor for mild steel corrosion in acidic medium, *Asian Journal of Chemistry*, **22**: 4537-4548.
13. M. A. Quraishi, S. Ambrish, S. Vinod Kumar, Y. Dileep Kumar, S. Ashish Kumar, (2010) Green approach to corrosion inhibition of mild steel in hydrochloric acid and sulphuric acid solutions by the extract of *Murraya koenigii* leaves, *Materials Chemistry and Physics*, **122**: 114-122.
14. S. Dontha, H. Kamurthy, B. Mantripragada, (2015) Phytochemical and pharmacological profile of *Ixora*: A review, *International Journal of Pharmaceutical Sciences and Research*, **7**: 567-584.
15. N. O. Obi-Egbedi, I. B. Obot, (2013) Xanthone: A new and effective corrosion inhibitor for mild steel in sulphuric acid solution, *Arabian Journal of Chemistry*, **6**: 211-223.
16. X. H. Li, S. D. Deng, H. Fu, G. N. Mu, (2009) Inhibition by tween-85 of the corrosion of cold rolled steel in 1.0 M hydrochloric acid solution, *Journal of Applied Electrochemistry*, **39**: 1125-1135.
17. I. N. Putilova, S. A. Balezin, V. P. Barannik, (1960) *Metallic Corrosion Inhibitors*, New York, USA: Pergamon Press.
18. S. Banerjee, V. Srivastava, M. M. Singh, (2012) Chemically modified natural polysaccharide as green corrosion inhibitor for mild steel in acidic medium, *Corrosion Science*, **59**: 35-41.
19. V. R. Saliyan, A. V. Adhikari, (2008) Inhibition of corrosion of mild steel in acid media by N'-benzylidene-3-(quinolin-4-ylthio) propanohydrazide, *Bulletin of Materials Science*, **31**: 699-711.
20. A. S. Fouda, S. H. Etaiw, W. Elnggar, (2014) Punica plant extract as green corrosion inhibitor for C-steel in hydrochloric acid solutions, *International Journal of Electrochemical Science*, **9**: 4866-4883.
21. M. F. Lebrini, F. Robert, C. Roos, (2010) Inhibition effect of alkaloids extract from *Annona squamosa* plant on the corrosion of C38 steel in normal hydrochloric acid medium, *International Journal of Electrochemical Science*, **5**: 1698-1712.
22. I. E. Uwah, P. C. Okafor, V. E. Ebiekpe, (2013) Inhibitive action of ethanol extracts from *Nauclea latifolia* on the corrosion of mild steel in H₂SO₄ solutions and their adsorption characteristics, *Arabian Journal of Chemistry*, **6**: 285-293.
23. G. Ji, S. K. Shukla, P. Dwivedi, S. Sundaram, R. Prakash, (2011) Inhibitive effect of *Argemone mexicana* plant extract on acid corrosion of mild steel, *Industrial and Engineering Chemistry Research*, **50**: 11954-11959.
24. G. Ji, S. K. Shukla, P. Dwivedi, S. Sundaram, E. E. Ebenso, R. Prakash, (2012) *Parthenium hysterophorus* Plant extract as an efficient green corrosion inhibitor for mild steel in acidic environment, *International Journal of Electrochemical Science*, **7**: 9933-9945.
25. A. Saxena, D. Prasad, R. Haldhar, G. Singh, A. Kumar, (2018) Use of *Saraca ashoka* extract as green corrosion inhibitor for mild steel in 0.5 M H₂SO₄, *Journal of Molecular Liquids*, **258**: 89-97.
26. O. Olivares-Xometl, N. V. Likhanova, M. A. Dominguez-Aguilar, E. Arce, H. Dorantes, P. Arellanes-Lozada, (2008) Synthesis and corrosion inhibition of α -amino acids alkylamides for mild steel in acidic environment, *Materials Chemistry and Physics*, **110**: 344-351.
27. M. R. Vinutha, T. V. Venkatesha, (2016) Review on mechanistic action of inhibitors on steel corrosion in acidic media, *Portugaliae Electrochimica Acta*, **34**: 157-184.
28. A. A. Begum, R. M. Vahith, V. Kotra, M. R. Shaik, A. Abdelgawad, E. M. Awwad, M. Khan, (2021) *Spilanthes acmella* leaves extract for corrosion inhibition in acid medium, *Coatings*, **11**: 106.

***Bibliographical Sketch**

Dr. A. Prithiba is an Assistant Professor in Avinashilingam Institute for Home Science and Higher Education for Women, Coimbatore, Tamil Nadu, India. Her research interests are Corrosion Science, Materials Chemistry. She has published 15 articles in National and International journals. She has guided 22 M.Sc. candidates and 2 M.Phil scholars. Currently, she is guiding 3 Ph.D scholars.



Dr. S. Manimegalai is an Assistant Professor in Arulmigu Palaniandavar College of Arts and Culture, Palani-624601, Dindigul District, and Tamil Nadu, India. Her research interests are Corrosion Chemistry, Phytochemistry, and Nano chemistry for the past 15 years. She has about 20 peer-reviewed, Scopus and Web of Science in National and International journal publications. He has published/presented in various National and International Seminars/Conferences pertaining to Corrosion Chemistry, Phytochemistry, and Nano chemistry. She has guided more than 20 M.Sc. candidates.